

Steam concentration cell using a high temperature type proton conductive solid electrolyte

H. UCHIDA, N. MAEDA, H. IWAHARA

Department of Environmental Chemistry and Technology, Faculty of Engineering, Tottori University, Koyamacho, Tottori 680, Japan

Received 27 January 1982

The concept of a steam concentration cell is discussed. A steam concentration cell was constructed using proton conductive solid electrolytes based on SrCeO_3 and the emf was measured under various conditions. Some characteristics of the cell on discharging are discussed. The electrode reactions in the cell were studied and the electroactive species at the anode was confirmed to be water molecules. The theoretical equation for the emf of the steam concentration cell is derived. Since conduction in the specimen oxides was not purely ionic but partially electronic, the proton transport numbers were determined from the emf of the cell under various conditions.

1. Introduction

In a recent paper [1] we reported that some sintered oxides based on SrCeO_3 exhibited proton conduction under a hydrogen-containing atmosphere at high temperatures. The applications of these materials as solid electrolytes for high temperature steam electrolysis and fuel cells have also been discussed [2, 3]. In these papers, we proposed the concept of a steam concentration cell using a high temperature type proton conductor [1].

When gases with different humidities were supplied to the electrode compartments of the gas cell with an electrolyte diaphragm based on SrCeO_3 ceramics, a distinct emf was observed; the electrode with a higher vapour pressure being negative. A stable and steady current could be drawn from the cell. Although this is a kind of gas concentration cell, the concept of a steam concentration cell has not yet been reported, probably, due to lack of appropriate proton conductive solids.

In the present study, the characteristics of steam concentration cells are examined using a SrCeO_3 -based proton conductor as the solid electrolyte, and the cell reaction is investigated under various conditions. Transport numbers of protons in this solid electrolyte are derived from the emf of the concentration cell.

2. Experimental procedures

The proton conductive solids used in this study were $\text{SrCe}_{1-x}\text{M}_x\text{O}_{3-\alpha}$ ($\text{M} = \text{Yb}, \text{Mg}; x = 0.05$ or 0.10), where α is the number of oxygen deficiencies per perovskite type oxide unit cell. The preparation of the specimens was the same as in the previous study [1]. The dense sinters obtained were sliced into thin discs (thickness, about 0.5 mm; diameter 12 mm) to provide test specimens.

The construction of the solid electrolyte gas cell Gas I, Pt/specimen disc/Pt, Gas II is illustrated in Fig. 1. The electrode compartments are separated by the solid electrolyte, each face of which is covered with porous platinum as an electrode material (projected electrode area: 0.5 cm^2). The cell temperature used was $600\text{--}1000^\circ \text{C}$. Air, oxygen, nitrogen, helium or mixtures of these gases were used at 1 atm as gas I or gas II.

The partial pressure of water vapour, $p_{\text{H}_2\text{O}}$, in the gases was controlled by saturating the water vapour at a given temperature to an accuracy of $\pm 1^\circ \text{C}$. Unless stated otherwise, the gas saturated with water vapour at room temperature is represented simply as wet gas (vapour pressure; 17–20 torr). Dry gas was prepared by passing through silica gel and phosphorous pentoxide.

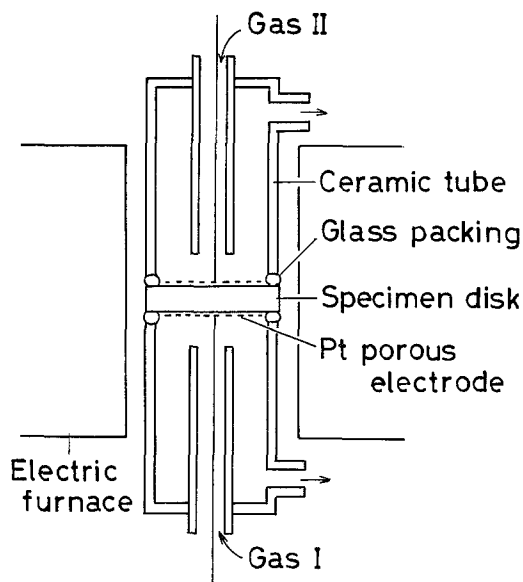


Fig. 1. Schematic illustration of a gas cell.

The partial pressure of oxygen, p_{O_2} , was measured with an oxygen meter which was an oxygen gas concentration cell using YSZ (yttria stabilized zirconia).

In order to test the discharge characteristics of the cell, a current pulse generator (Hokuto Denko, Model HC-110) and a digital memory scope (Hitachi, Model VC-801L) were employed.

3. Results and discussion

3.1. Steam concentration cell

Typical examples of emf values for various gas cells are shown in Table 1. When dry air was introduced into both electrode compartments (cell 1 in Table 1), the emf observed was nearly zero

because there is no difference in the partial pressures of oxygen or water vapour experienced by the electrodes.

However, when wet air instead of dry air was introduced into one of the electrode compartments (cell 2 in Table 1), a build-up of emf was observed as shown in Fig. 2. After a few minutes, the emf of cell 2 reached a stable value. In this cell, the electrode with the higher humidity was negative. The emf of the cell responded to the vapour pressure difference between the two electrode gases as shown in Table 2. This can be regarded as a sort of steam concentration cell with a proton conductive solid electrolyte.

As reported previously [1], the cell did not act as an oxygen concentration cell (cell 3 in Table 1) when dry gases were used. The conduction in that case was electronic due to electron holes present in the oxides [1].

A steady and stable current could be drawn from the steam concentration cell. During discharge at a constant current density, the terminal voltage was very stable and no deterioration was observed even after 2 days of continuous discharge (Fig. 3). Response to the current pulse was rapid as shown in Fig. 4. Since the instantaneous voltage drop after current interruption is taken as the IR drop, it was suggested that the ohmic polarization was predominant in this cell. This agreed with the experimental data from the discharge curves shown in Fig. 5. The relationship between the terminal voltage and the current output are linear in this cell. From the slope of the discharge curve, d.c. resistances of the cells were calculated to be 21Ω at 800°C and 6.5Ω at 1000°C . On the other hand, the resistances of the cell measured by a 10 kHz a.c. bridge were 16.2Ω at 800°C and

Table 1. Emf of gas cells, gas I, Pt/specimen oxide/Pt, gas II

Cell number	Cell type* gas I//gas II	Emf (mV) [†]			
		SrCe _{0.95} Yb _{0.05} O _{3-α}		SrCe _{0.90} Yb _{0.10} O _{3-α}	
		600° C	800° C	600° C	800° C
1	dry air//dry air	0.0	-0.5	0.0	0.0
2	wet air//dry air	59.0	30.0	76.0	40.0
3	dry air//dry O ₂	0.5	1.0	0.0	0.0

* Dry gas dried with silica gel and P₂O₅; wet gas, saturated with H₂O at room temperature (21–22° C).

[†] Negative sign shows that the electrode of gas II is negative.

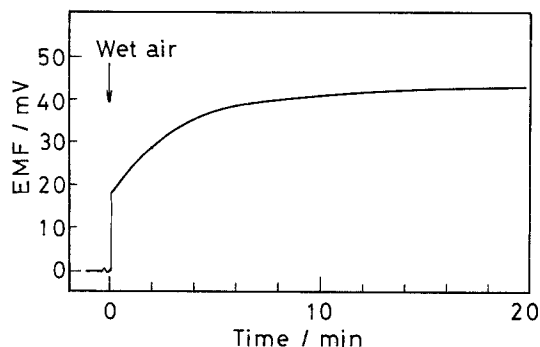
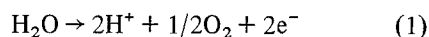


Fig. 2. Build-up of the emf on introducing wet air to one of the electrode compartments (cell 2) at 800°C. Electrolyte: $\text{SrCe}_{0.95}\text{Yb}_{0.05}\text{O}_{3-\alpha}$.

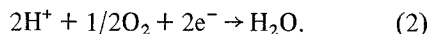
5.8Ω at 1000°C. Although the d.c. resistance of the cell was somewhat higher than the a.c. value, the resistance of the solid electrolyte was a major factor in the voltage drop for the cell and the electrode reactions can be considered to occur reversibly.

The cell behaviour described above can be rationally explained by assuming that the specimen has proton conduction in the moistened atmosphere [1]. If the diaphragm in cell 2 is a proton conductor, the difference in the partial pressure of water vapour ($p_{\text{H}_2\text{O}}$) between the two electrodes can be a driving force for the following electrode reactions:

Electrode with higher $p_{\text{H}_2\text{O}}$



electrode with lower $p_{\text{H}_2\text{O}}$



For this reason, this cell may give a stable emf,

Table 2. Emf response of the cell: wet air, $p_{\text{H}_2\text{O}}(I)$ /
 $\text{SrCe}_{0.95}\text{Yb}_{0.05}\text{O}_{3-\alpha}$ /dry air ($p_{\text{H}_2\text{O}} = 4.6 \text{ torr}$) to the change
in $p_{\text{H}_2\text{O}}(I)$

$p_{\text{H}_2\text{O}}(I)$ (torr)	Emf (mV)			
	600°C		800°C	
	E	E_0	E	E_0
4.6	0.0	0.0	0.0	0.0
12.8	17.8	38.4	11.0	47.3
23.8	39.5	61.8	26.0	76.0
42.2	52.5	83.4	31.4	102.5

E_0 : theoretical emf calculated from Equation 3.

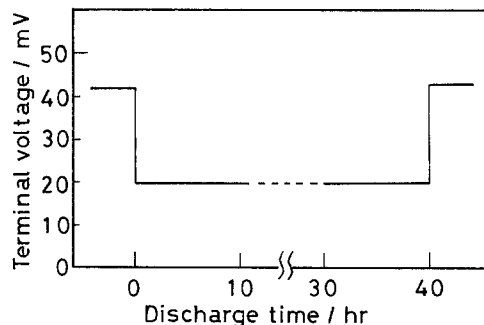


Fig. 3. Continuous discharge test of the cell: wet air/dry air, at constant current density of 2 mA cm^{-2} . Electrolyte: $\text{SrCe}_{0.95}\text{Yb}_{0.05}\text{O}_{3-\alpha}$; cell temperature: 800°C.

with the electrode at the lower $p_{\text{H}_2\text{O}}$ being the cathode.

In order to verify the above reactions, we checked the oxygen evolution or consumption at the electrodes during discharge of the cell as illustrated schematically in Fig. 6a. In this case, dry and wet helium was supplied to each electrode compartment at a regulated flow rate ($1 \text{ cm}^3 \text{ s}^{-1}$). The electrode diaphragm used was $\text{SrCe}_{0.95}\text{Yb}_{0.05}\text{O}_{3-\alpha}$. The emf of the cell was 108 mV at 800°C. The partial pressure of oxygen in the wet gas was monitored at the outlet of the cell using a YSZ oxygen meter kept at 800°C.

When this cell was short-circuited, a current of $287 \mu\text{A}$ was observed and the increase in p_{O_2} in the wet helium at the outlet of the anode compartment was detected by the emf of a YSZ oxygen meter (Fig. 6b). On opening the circuit, the p_{O_2} rapidly returned to the original value. At the outlet of the cathode compartment, the inverse response (decrease in p_{O_2} in dry helium on short-circuiting) was observed. Thus, we could confirm

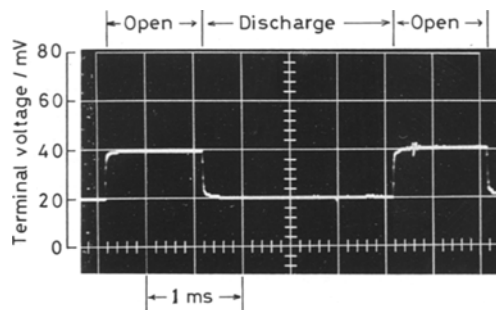


Fig. 4. Typical transient behaviour on switching current on and off the cell: wet air/ $\text{SrCe}_{0.95}\text{Yb}_{0.05}\text{O}_{3-\alpha}$ /dry air, at 800°C, OCV = 40 mV, discharge current = 2 mA cm^{-2} .

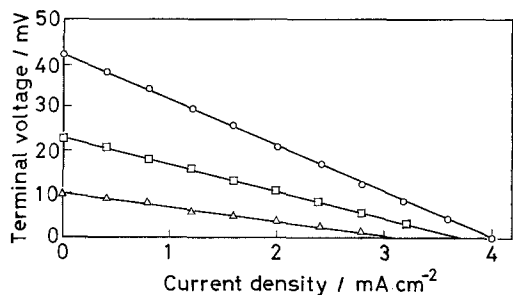


Fig. 5. Performances of the cell: wet air/
 $\text{SrCe}_{0.95}\text{Yb}_{0.05}\text{O}_{3-\alpha}$ /dry air. \circ : 800°C, \square : 900°C,
 \triangle : 1000°C.

the oxygen evolution at the anode and consumption at the cathode while discharging the cell. These results support the validity of the electrode reactions 1 and 2 above.

From thermodynamic, electrochemical consideration of Equations 1 and 2, we can derive the theoretical emf of the steam concentration cell. Generally, when gas I and gas II in the cell include oxygen and water vapour at different partial pressures, the emf, E , of the cell can be given as

$$E = \frac{RT}{2F} \ln \left[\frac{p_{\text{H}_2\text{O}}(\text{I})}{p_{\text{H}_2\text{O}}(\text{II})} \right] \left[\frac{p_{\text{O}_2}(\text{II})}{p_{\text{O}_2}(\text{I})} \right]^{1/2} \quad (3)$$

where R , F and T have their usual meanings.

Further experiments to measure the emf were carried out and the results are shown in Table 3. A stable emf was also observed when the two electrode gases had different oxygen partial pressures but equal vapour pressures, like cell 4

in Table 3. This is reasonable since the emf of cell 4 can be written according to Equation 3 as

$$E = \frac{RT}{4F} \ln \frac{p_{\text{O}_2}(\text{II})}{p_{\text{O}_2}(\text{I})} \quad (4)$$

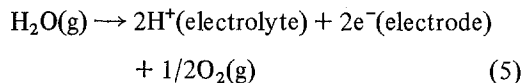
when $p_{\text{H}_2\text{O}}(\text{I}) = p_{\text{H}_2\text{O}}(\text{II})$

This is a 'wet' oxygen concentration cell (cf. cell 3 in Table 1). Cells 5 and 6 show that the electrodes with higher humidity are again negative, and that the absolute emf values at 600°C are higher than those oxygen concentration cells (29.5 mV at 600°C). Similarly, the emf behaviour of cells 5 and 6 can be explained qualitatively by Equation 3.

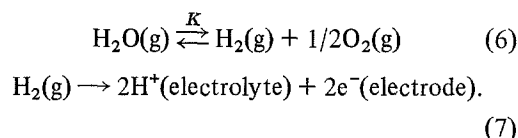
3.2. Electroactive species at the anode

For the formation of protons at the anode, two distinguishable reaction models are possible.

Model 1



Model 2



In model 1, protons are extracted directly from water molecules at the anode. In model 2, hydrogen molecules, which are produced by thermal dissociation equilibrium (Equation 6), are

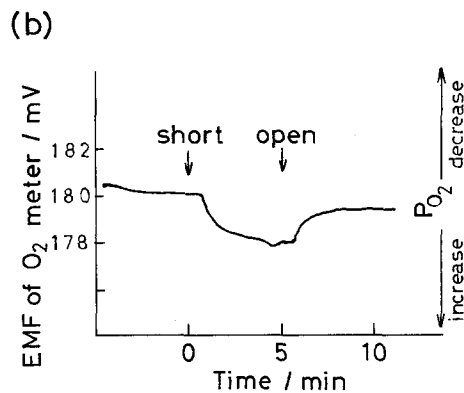
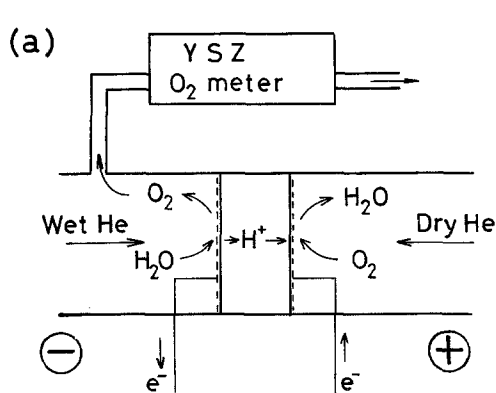


Fig. 6. Experimental confirmation of the oxygen evolution at the anode of the steam concentration cell. (a) Schematic illustration of the steam concentration cell reaction. Concept and method for oxygen detection. (b) Change in the p_{O_2} in wet helium detected by the emf response of the YSZ oxygen meter.

Table 3. *Emf of gas cells, gas I, Pt/specimen oxide/Pt, gas II*

Cell number	Cell type* gas I//gas II	Emf (mV) [†]			
		SrCe _{0.95} Yb _{0.05} O _{3-α}		SrCe _{0.90} Yb _{0.10} O _{3-α}	
		600° C	800° C	600° C	800° C
4	wet air//wet O ₂	25.0	14.0	16.0	12.0
5	wet air//dry O ₂	69.5	30.5	46.8	19.5
6	dry air//wet O ₂	-43.5	-13.0	-25.0	-10.5

* Dry gas, dried with silica gel and P₂O₅; wet gas, saturated with H₂O at room temperature (21–22° C).

[†] Negative sign shows that the electrode of gas II is negative.

ionized to protons at the anode. Which model is more valid?

As shown in Fig. 5, quite a high current (4 mA cm⁻²) could be drawn from the steam concentration cell at 800° C. Considering the two-electron reaction for the ionization of one water molecule or one hydrogen molecule, the rate of consumption at the anode was 1.25 × 10¹⁶ molecules s⁻¹ cm⁻². Assuming that only the molecules which collide with the electrode plane (wall) could be ionized to protons, the number of molecules supplied to the electrode was estimated as follows.

The mean velocity of a molecule, \bar{c} , is given by

$$\bar{c} = \left(\frac{8RT}{\pi M} \right)^{1/2} \text{ (cm s}^{-1}\text{)} \quad (8)$$

where M is molecular weight. The rate of collision of the molecules with a wall per unit area, Z , is given by

$$Z = 1/4 N \bar{c} \text{ (molecules s}^{-1}\text{ cm}^{-2}\text{)} \quad (9)$$

where N is the number of molecules per unit volume.

The equilibrium partial pressure of hydrogen in the experimental condition calculated from the dissociation constant K [4] is $p_{\text{H}_2} = 4.49 \times 10^{-11}$ atm. Using this value, \bar{c}_{H_2} and Z_{H_2} are calculated as

$$\bar{c}_{\text{H}_2} = 3.37 \times 10^5 \text{ cm s}^{-1}$$

$$Z_{\text{H}_2} = 2.59 \times 10^{13} \text{ molecules s}^{-1}\text{ cm}^{-2}.$$

For water vapour ($p_{\text{H}_2\text{O}} = 2.63 \times 10^{-2}$ atm), these values are

$$\bar{c}_{\text{H}_2\text{O}} = 1.12 \times 10^5 \text{ cm s}^{-1}$$

$$Z_{\text{H}_2\text{O}} = 5.04 \times 10^{21} \text{ molecules s}^{-1}\text{ cm}^{-2}.$$

The consumption rate by the discharge current is higher than the rate of supply of hydrogen to the electrode by a factor of 500. Although the gas flow rate (1 cm³ s⁻¹) was completely neglected in these calculations, the values of Z might be somewhat higher in the actual cell. At 1000° C, the equilibrium constant K is about two orders of magnitude higher than that at 800° C. However, even though the rate of supply of hydrogen became comparable to that of consumption, a considerable concentration polarization should occur on discharging the cell. Such polarization could not be observed as described above.

On the other hand, water molecules are supplied to the electrode in sufficient quantity at the temperatures examined (about 6 orders of magnitude over the consumption rate) so that the number of molecules consumed at the electrode can be neglected.

Therefore, the species ionized at the anode of this steam concentration cell must be water molecules (Equation 5) and not hydrogen molecules (Equation 7).

3.3. Proton transport numbers of SrCe_{0.95}Yb_{0.05}O_{3-α}

As shown in Table 2, the observed emf values of the steam concentration cells were generally lower than the value calculated from Equation 3. This shows that the conduction in the ceramics is not purely ionic but partially electronic.

In order to determine the proton transport numbers, t_{H^+} , in the specimens, the emf values of the following steam concentration cells were measured. The pressures of water vapour added to each electrode gas were 23.8 and 4.6 torr, corre-

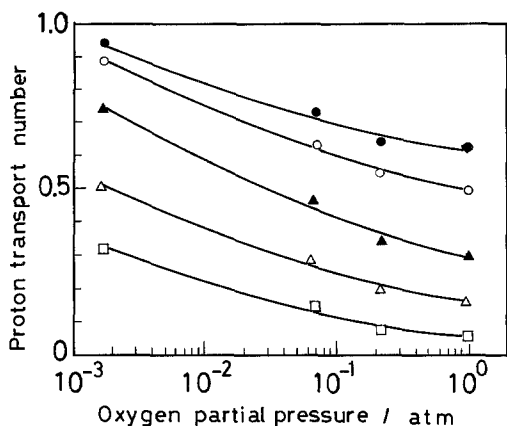


Fig. 7. Dependence of the proton transport number on the oxygen partial pressure. Specimen: $\text{SrCe}_{0.95}\text{Yb}_{0.05}\text{O}_{3-\alpha}$. ●: 600° C, ○: 700° C, ▲: 800° C, △: 900° C, □: 1000° C.

sponding to the vapour pressures at 25 and 0° C, respectively. And the oxygen partial pressures at both electrodes were kept at the same value.

When $p_{\text{O}_2}(\text{I}) = p_{\text{O}_2}(\text{II})$, according to Equation 3, the theoretical emf of the cell is given by

$$E_0 = \frac{RT}{2F} \ln \frac{p_{\text{H}_2\text{O}}(\text{I})(= 23.8 \text{ torr})}{p_{\text{H}_2\text{O}}(\text{II})(= 4.6 \text{ torr})} \quad (10)$$

and t_{H^+} was determined to be E/E_0 .

Figure 7 shows the proton transport numbers of $\text{SrCe}_{0.95}\text{Yb}_{0.05}\text{O}_{3-\alpha}$ at 600–1000° C. When nitrogen gas ($p_{\text{O}_2} = 1.7 \times 10^{-3}$ atm) was used, the proton transport number was about unity at 600° C. However, with an increase in p_{O_2} , t_{H^+} decreases. Such experimental facts could be rationally explained by a mechanism of proton conduction as proposed in a previous study [1]. Decreases in t_{H^+} with increases in p_{O_2} might be ascribed to the increases in hole conduction in the specimen oxide. Electron holes surviving in the oxides might make t_{H^+} decrease.

Although the t_{H^+} in the specimen under wet air decreased at higher temperatures, the t_{H^+} was about 0.95 at 800° C for H_2 – O_2 fuel cells [1]. Furthermore, in the steam electrolysis cells to produce hydrogen with SrCeO_3 -based electrolytes, the current efficiencies were about 0.9 at 700–900° C [1, 2]. These facts suggest that the t_{H^+} may

become much higher in the steam concentration cell if the gas with higher $p_{\text{H}_2\text{O}}$, which results in higher p_{H_2} and lower p_{O_2} , is used as the anode gas. Detailed studies of proton conduction in SrCeO_3 -based sinters are in progress.

4. Conclusion

A steam concentration cell could be constructed using the high temperature proton conductor $\text{SrCe}_{1-x}\text{M}_x\text{O}_{3-\alpha}$ at 600 to 1000° C. When gases with different humidities were supplied to the electrode compartments of the gas cells with these electrolytes, a distinct emf was observed, the electrode of higher vapour pressure being negative. The resistance of the specimen electrolyte was the major factor determining the voltage drop in the discharging cell and the electrode reactions occur reversibly.

From the analysis of the change in p_{O_2} in the electrode gas on short-circuiting the cell, the electrode reactions were confirmed to be those of Equations 1 and 2. It was also clarified that, at the anode, protons are extracted directly from water molecules, and that the contribution of hydrogen molecules produced by the thermal dissociation equilibrium is negligible as electroactive species at the anode.

Based on Equations 1 and 2, the theoretical emf of the steam concentration cell was derived, and emf behaviour of this cell could be rationally explained by this equation. As the conductions in the ceramics were not purely ionic but partially electronic, the proton transport number, t_{H^+} , in the specimen was determined from the emf. The t_{H^+} increased with decreasing p_{O_2} and with decreasing temperature.

The steam concentration cell may be applied, in principle, to the high temperature type humidity sensor and the recovery of energy from exhaust gas from large-scale burner in the industrial plants. In the former case, the pressure of water vapour can be known from the emf of the cell, if the partial pressure of water vapour at one electrode and the partial pressure of oxygen at both electrodes are known. This type of sensor has the

possibility of serving as a check and control device for water vapour. We are now investigating the characteristics of this galvanic cell type humidity sensor.

References

- [1] H. Iwahara, T. Esaka, H. Uchida and N. Maeda, *J. Solid State Ionics* 3/4 (1981) 359.
- [2] H. Iwahara, H. Uchida and N. Maeda, *J. Power Sources* 7 (1982) 293.
compiled by C. J. West, McGraw-Hill, New York (1930).
- [3] H. Iwahara, H. Uchida and T. Esaka, *Prog. Batteries Solar Cells* 4 (1982) 279.
- [4] 'International Critical Tables' Vol. VII, p. 231,